

# Implementación de simuladores realistas de dispositivos DG-MOSFET a nanoescala en plataformas de altas prestaciones

María José Cáceres Granados, Andrés Godoy Medina, José Miguel Mantas Ruiz, Carlos Sampetro Matarín, Francesco Vecil

Granada, 12 July 2011

# Outline

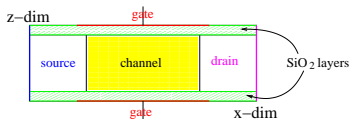
- 1 The model
  - Introduction
  - Modelling
- 2 Numerical schemes
  - Iterative schemes for the Schrödinger-Poisson block
  - Solvers for Schrödinger and Poisson
  - Numerical methods for the BTE
  - Parallelization
- 3 Experiments
  - Newton vs. Gummel
  - Equilibria
  - Time-dependent simulations
  - Plasma oscillations (from the one-valley solver)

# Outline

- 1 The model
  - Introduction
  - Modelling
- 2 Numerical schemes
  - Iterative schemes for the Schrödinger-Poisson block
  - Solvers for Schrödinger and Poisson
  - Numerical methods for the BTE
  - Parallelization
- 3 Experiments
  - Newton vs. Gummel
  - Equilibria
  - Time-dependent simulations
  - Plasma oscillations (from the one-valley solver)

# Geometry

We afford the simulation of a nanoscaled MOSFET.



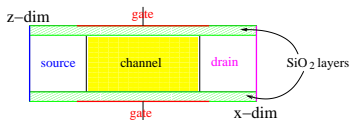
## About the scaling

In 1971, the Intel 4004 processor had 1000 transistors, whose channel length was 10000 nm. In 1974, the Intel 8008 processor had 6-7 thousand. In 2003 the Intel Pentium IV had 50 million. Nowadays processors may have 400 million transistors, whose channel is 28 nm long.

## Why is it important?

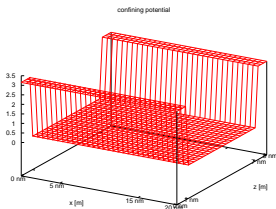
Smaller MOSFETs allow for the construction of smaller devices with better performances; moreover, they allow silicon and energy saving, due to the lower source-drain potential drop needed to switch on or off the transistor.

# Geometry



## The role of the insulating layers

Electrons are trapped inside a potential well of width 6 nm (comparable to the Debye length) and of depth 3.15 V along the  $z$ -dimension.



This leads to quantization of energy.

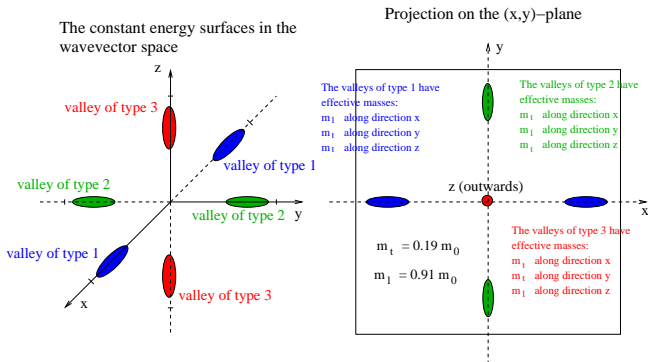
# Outline

- 1 The model
  - Introduction
  - **Modelling**
- 2 Numerical schemes
  - Iterative schemes for the Schrödinger-Poisson block
  - Solvers for Schrödinger and Poisson
  - Numerical methods for the BTE
  - Parallelization
- 3 Experiments
  - Newton vs. Gummel
  - Equilibria
  - Time-dependent simulations
  - Plasma oscillations (from the one-valley solver)

# Band structure

## The three valleys

The Si band structure presents six minima in the first Brillouin zone:



The axes of the ellipsoids are disposed along the  $x$ ,  $y$  and  $z$  axes of the reciprocal lattice. The three minima have the same value, therefore there is no gap.

# Band structure

## Non-parabolicity

The band structure around the three minima can be expanded following the Kane non-parabolic approximation ( $\nu$  indexes the valley):

$$\epsilon_{\nu}^{kin}(k_x, k_y) = \frac{\hbar^2}{1 + \sqrt{1 + 2\tilde{\alpha}_{\nu}\hbar^2 \left( \frac{k_x^2}{m_e m_{x,\nu}} + \frac{k_y^2}{m_e m_{y,\nu}} \right)}} \left( \frac{k_x^2}{m_e m_{x,\nu}} + \frac{k_y^2}{m_e m_{y,\nu}} \right),$$

where  $m_{x,\nu}$  and  $m_{y,\nu}$  are the effective masses along the unconfined dimensions and the  $\tilde{\alpha}_{\nu}$  are the Kane dispersion factors.

## $z$ -direction

The band structure does not depend on  $z$  as the carriers are not free to move along that direction.

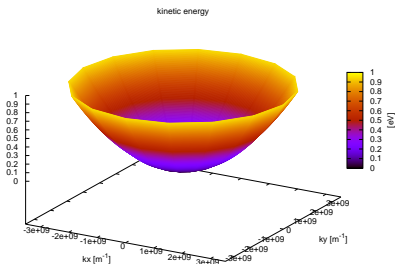
## Electron population

The total amount of carriers is split into independent populations, one for each valley. We shall index them  $\nu = 1, 2, 3$ .

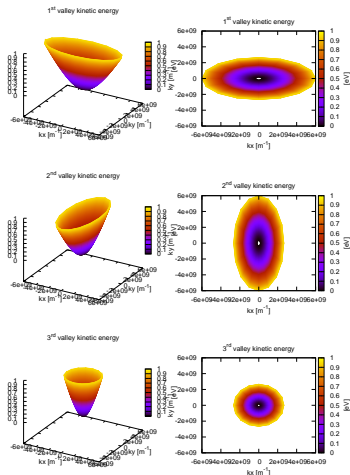


# Band structure

## One-valley approximation vs. three-valley approximation



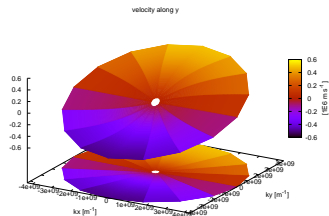
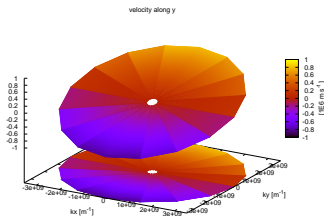
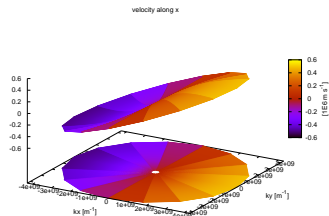
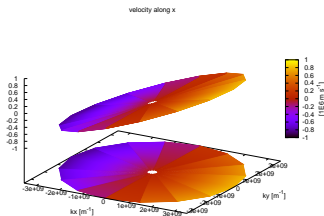
(a)  $\epsilon^{kin}$  with  $\tilde{\alpha} = 0$



(b)  $\epsilon_{\nu}^{kin}$  with  $\tilde{\alpha}_{\nu} = 0$

# Band structure

## Parabolic vs. non-parabolic

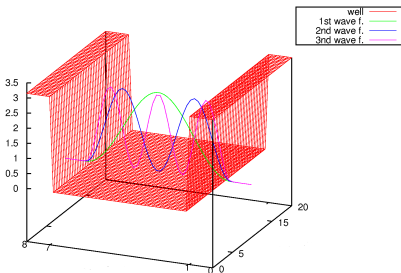


(c)  $v_x$  and  $v_y$  with  $\tilde{\alpha} = 0$

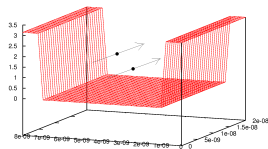
(d)  $v_x$  and  $v_y$  with  $\tilde{\alpha} = 0.5$

# Dimensional coupling

Justified because  $z$ -dim. is quasi-static with respect to  $x$ -dim.



(e)  $z$ -dimension: waves



(f)  $x$ -dimension: particles

# The confinement

## Description of the confinement

A set of 1D Schrödinger eigenvalue problems describe the electrons along  $z$ .

$$-\frac{\hbar^2}{2} \frac{d}{dz} \left[ \frac{1}{m_{z,\nu}} \frac{d\chi_{\nu,p}[V]}{dz} \right] - q(V + V_c) \chi_{\nu,p}[V] = \epsilon_{\nu,p}[V] \chi_{\nu,p}[V]$$

## Subbands

The eigenvalues  $\{\epsilon_{\nu,p}\}_{p=1}^{\infty}$  represent the energy levels, called *subbands* in physics.

## Wave functions

The eigenvectors  $\{\chi_{\nu,p}(\cdot)\}_{p=1}^{\infty}$  are called *wave functions* in physics.

## Electron population

The subbands decompose the electron population of the  $\nu^{\text{th}}$  valley into independent populations. The densities are indexed on the pair  $(\nu, p)$ .

# The unconfined dimension

## BTE

The Boltzmann Transport Equation (one for each pair  $(\nu, p)$ ) reads

$$\frac{\partial f_{\nu,p}}{\partial t} + \frac{1}{\hbar} \nabla_k \epsilon_{\nu}^{kin} \cdot \nabla_x f_{\nu,p} - \frac{1}{\hbar} \nabla_x \epsilon_{\nu,p} \cdot \nabla_k f_{\nu,p} = \mathcal{Q}_{\nu,p}[f], \quad f_{\nu,p}(t=0) = \rho_{\nu,p}^{eq} M_{\nu}.$$

## The collision operator

Electrons are scattered by the vibration of the crystal lattice, described as phonons:

$$\mathcal{Q}_{\nu,p}[f] = \sum_s \sum_{\nu',p'} \int_{\mathbb{R}^2} [\mathcal{S}_{(\nu',p',k') \rightarrow (\nu,p,k)}^s f_{\nu',p'}(k') - \mathcal{S}_{(\nu,p,k) \rightarrow (\nu',p',k')}^s f_{\nu,p}(k)] dk'.$$

## The electrostatic potential

Electrons are driven by the applied bias:

$$-\text{div}_{x,z} [\epsilon_R \nabla_{x,z} V] = -\frac{q}{\epsilon_0} (N - N_D).$$

# Eigenstates, mixed states and classical states.

The classical states are the magnitudes which only depend on the unconfined dimension  $x$ , while mixed states depend on both  $x$  and  $z$ .

## Eigenstates

The subbands and the wave functions  $\{\epsilon_{\nu,p}(x), \chi_{\nu,p}(x, \cdot)\}_{p=1}^{\infty}$  are eigenstates; they depend on  $x$  only as a parameter.

## Mixed states

The electrostatic potential  $V(x, z)$  and the volume density  $N(x, z) = 2 \sum_{\nu=1}^3 \sum_{p=1}^{\infty} \int_{\mathbb{R}^2} f_{\nu,p}(t, x, k) dk |\chi_{\nu,p}(x, z)|^2$  are mixed states.

## Classical states

The pdf's  $\{f_{\nu,p}(t, x, k_x, k_y)\}_{\nu,p}$  are classical states, therefore the surface density

$$\rho(x) = 2 \sum_{\nu=1}^3 \sum_{p=1}^{\infty} \int_{\mathbb{R}^2} f_{\nu,p}(t, x, k) dk$$

is a classical state too, and in general most of the macroscopic magnitudes.

# The model

## BTE

The Boltzmann Transport Equation (one for each subband and for each valley) reads

$$\frac{\partial f_{\nu,p}}{\partial t} + \frac{1}{\hbar} \nabla_k \epsilon_{\nu}^{kin} \cdot \nabla_x f_{\nu,p} - \frac{1}{\hbar} \nabla_x \epsilon_{\nu,p} \cdot \nabla_k f_{\nu,p} = \mathcal{Q}_{\nu,p}[f], \quad f_{\nu,p}(t=0) = \rho_{\nu,p}^{eq} M_{\nu}.$$

## Schrödinger-Poisson block

$$-\frac{\hbar^2}{2} \frac{d}{dz} \left[ \frac{1}{m_{z,\nu}} \frac{d\chi_{\nu,p}[V]}{dz} \right] - q(V + V_c) \chi_{\nu,p}[V] = \epsilon_{\nu,p}[V] \chi_{\nu,p}[V]$$

$$-\text{div}_{x,z} [\epsilon_R \nabla_{x,z} V] = -\frac{q}{\epsilon_0} \left( 2 \sum_{\nu,p} \rho_{\nu,p} |\chi_{\nu,p}[V]|^2 - N_D \right)$$

These equations cannot be decoupled because we need the **eigenfunctions** to compute the potential (in the expression of the **total density**), and we need the potential to compute the eigenfunctions.

# The model

## BTE

The Boltzmann Transport Equation (one for each subband and for each valley) reads

$$\frac{\partial f_{\nu,p}}{\partial t} + \frac{1}{\hbar} \nabla_k \epsilon_{\nu}^{kin} \cdot \nabla_x f_{\nu,p} - \frac{1}{\hbar} \nabla_x \epsilon_{\nu,p} \cdot \nabla_k f_{\nu,p} = \mathcal{Q}_{\nu,p}[f], \quad f_{\nu,p}(t=0) = \rho_{\nu,p}^{eq} M_{\nu}.$$

## Schrödinger-Poisson block

$$-\frac{\hbar^2}{2} \frac{d}{dz} \left[ \frac{1}{m_{z,\nu}} \frac{d\chi_{\nu,p}[V]}{dz} \right] - q(V + V_c) \chi_{\nu,p}[V] = \epsilon_{\nu,p}[V] \chi_{\nu,p}[V]$$

$$-\text{div}_{x,z} [\epsilon_R \nabla_{x,z} V] = -\frac{q}{\epsilon_0} \left( 2 \sum_{\nu,p} \rho_{\nu,p} |\chi_{\nu,p}[V]|^2 - N_D \right)$$

These equations cannot be decoupled because we need the **eigenfunctions** to compute the potential (in the expression of the **total density**), and we need the potential to compute the eigenfunctions.



# The model

## The collision operator

The collision operator takes into account the phonon scattering mechanism. It reads

$$\mathcal{Q}_{\nu,p}[f] = \sum_s \sum_{\nu',p'} \int_{\mathbb{R}^2} [S_{(\nu',p',k') \rightarrow (\nu,p,k)}^s f_{\nu',p'}(k') - S_{(\nu,p,k) \rightarrow (\nu',p',k')}^s f_{\nu,p}(k)] dk'.$$

## Structure of the $S^s$

The missing dimension of the wave-vector  $k \in \mathbb{R}^2$ , instead of  $k \in \mathbb{R}^3$ , is replaced by an overlap integral  $W_{(\nu,p),(\nu',p')}$ :

$$S_{(\nu,p,k) \rightarrow (\nu',p',k')}^s = C_{\nu \rightarrow \nu'} \frac{1}{W_{(\nu,p),(\nu',p')}} \delta(\epsilon_{\nu',p'}^{\text{tot}}(k') - \epsilon_{\nu,p}^{\text{tot}}(k) \pm \text{some energy})$$

$$\frac{1}{W_{(\nu,p),(\nu',p')}} = \int_0^{l_z} |\chi_{\nu,p}|^2 |\chi_{\nu',p'}|^2 dz, \quad [W] = m.$$

# The model

## The collision operator

The collision operator takes into account the phonon scattering mechanism. It reads

$$\mathcal{Q}_{\nu,p}[f] = \sum_s \sum_{\nu',p'} \int_{\mathbb{R}^2} [S_{(\nu',p',k') \rightarrow (\nu,p,k)}^s f_{\nu',p'}(k') - S_{(\nu,p,k) \rightarrow (\nu',p',k')}^s f_{\nu,p}(k)] dk'.$$

## Structure of the $S^s$

The missing dimension of the wave-vector  $k \in \mathbb{R}^2$ , instead of  $k \in \mathbb{R}^3$ , is replaced by an overlap integral  $W_{(\nu,p),(\nu',p')}$ :

$$S_{(\nu,p,k) \rightarrow (\nu',p',k')}^s = C_{\nu \rightarrow \nu'} \frac{1}{W_{(\nu,p),(\nu',p')}} \delta(\epsilon_{\nu',p'}^{\text{tot}}(k') - \epsilon_{\nu,p}^{\text{tot}}(k) \pm \text{some energy})$$

$$\frac{1}{W_{(\nu,p),(\nu',p')}} = \int_0^{l_z} |\chi_{\nu,p}|^2 |\chi_{\nu',p'}|^2 dz, \quad [W] = m.$$

# Initial condition

## Strategy

We want to initialize the system under the following constraints:

- let the potential in the corners float to the proper non-zero value;
- fulfill electrical neutrality at the source contact (symmetrically for the drain contact):

$$\int_0^{L_z} N_D(0, z) = \int_0^{L_z} N(0, z);$$

- have a thermodynamical equilibrium for the system, i.e. a distribution which is a zero for both the BTE and the scattering operator.



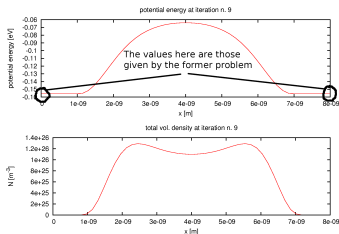
# Initial condition

## Step 2: the profile at the contacts

Solve a 1D Schrödinger-Poisson problem for the following density:

$$N[V] = \frac{\int_0^{L_z} N_D(0, z) dz}{\sum_{\nu', p'} \sqrt{m_{x, \nu'} m_{y, \nu'}} e^{-\frac{\epsilon_{\nu', p}[V](0)}{\kappa_B T L}}} \sum_{\nu, p} \sqrt{m_{x, \nu} m_{y, \nu}} e^{-\frac{\epsilon_{\nu, p}[V](0)}{\kappa_B T L}} |\chi_{\nu, p}[V](0, z)|^2$$

with homogeneous Neumann boundary conditions at  $z = 0$  and  $z = L_z$ . Moreover, impose  $V(0, 0) = V_{gap}$ . We retain the profile of  $V$  at the contacts:  $V_{border}(z) = V(0, z)$ .



# Initial condition

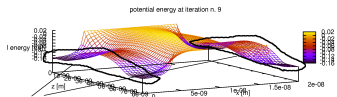
## Step 3: the thermodynamical equilibrium

Solve Schrödinger-Poisson problem for the following density:

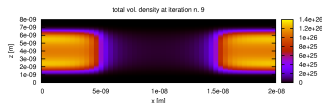
$$N[V] = \frac{\int_0^{L_z} N_D(0, z) dz}{\sum_{\nu', p'} \sqrt{m_{x, \nu} m_{y, \nu}} e^{-\frac{\epsilon_{\nu, p}[V_{border}]}{\kappa_B T_L}}} \sum_{\nu, p} \sqrt{m_{x, \nu} m_{y, \nu}} e^{-\frac{\epsilon_{\nu, p}[V](x)}{\kappa_B T_L}} |\chi_{\nu, p}[V](x, z)|^2$$

with Dirichlet conditions at the four metallic contacts and gates, homogeneous

Neumann elsewhere. Now the surface densities are of the form  $\rho_{\nu, p}^{eq} = C e^{-\frac{\epsilon_{\nu, p}(x)}{\kappa_B T_L}}$  and are, therefore, a zero for both Boltzmann and the scattering operator.



These profiles come from the solution of the 1D problem



# Outline

- 1 The model
  - Introduction
  - Modelling
- 2 Numerical schemes
  - **Iterative schemes for the Schrödinger-Poisson block**
  - Solvers for Schrödinger and Poisson
  - Numerical methods for the BTE
  - Parallelization
- 3 Experiments
  - Newton vs. Gummel
  - Equilibria
  - Time-dependent simulations
  - Plasma oscillations (from the one-valley solver)

# The Newton scheme

## The functional

Solving the Schrödinger-Poisson block

$$-\frac{\hbar^2}{2} \frac{d}{dz} \left[ \frac{1}{m_{z,\nu}} \frac{d\chi_{\nu,p}[V]}{dz} \right] - q(V + V_c) \chi_{\nu,p}[V] = \epsilon_{\nu,p}[V] \chi_{\nu,p}[V]$$

$$-\text{div} [\epsilon_R \nabla V] = -\frac{q}{\epsilon_0} (N[V] - N_D)$$

is equivalent to minimizing, under the constraints of the Schrödinger equation, the functional  $P[V]$

$$P[V] = -\text{div} (\epsilon_R \nabla V) + \frac{q}{\epsilon_0} (N[V] - N_D),$$

## The scheme

which is achieved by means of a Newton-Raphson iterative scheme

$$dP(V^{old}, V^{new} - V^{old}) = -P[V^{old}].$$



# The Newton scheme

## The functional

Solving the Schrödinger-Poisson block

$$-\frac{\hbar^2}{2} \frac{d}{dz} \left[ \frac{1}{m_{z,\nu}} \frac{d\chi_{\nu,p}[V]}{dz} \right] - q(V + V_c) \chi_{\nu,p}[V] = \epsilon_{\nu,p}[V] \chi_{\nu,p}[V]$$

$$-\operatorname{div} [\epsilon_R \nabla V] = -\frac{q}{\epsilon_0} (N[V] - N_D)$$

is equivalent to minimizing, under the constraints of the Schrödinger equation, the functional  $P[V]$

$$P[V] = -\operatorname{div} (\epsilon_R \nabla V) + \frac{q}{\epsilon_0} (N[V] - N_D),$$

## The scheme

which is achieved by means of a Newton-Raphson iterative scheme

$$dP(V^{old}, V^{new} - V^{old}) = -P[V^{old}].$$

# The iterations

## Derivatives

The Gâteaux-derivatives of the eigenproperties are needed:

$$d\epsilon_{\nu,p}(V, U) = -q \int U(\zeta) |\chi_{\nu,p}[V](\zeta)|^2 d\zeta$$

$$d\chi_{\nu,p}(V, U) = -q \sum_{p' \neq p} \frac{\int U(\zeta) \chi_{\nu,p}[V](\zeta) \chi_{\nu,p'}[V](\zeta) d\zeta}{\epsilon_{\nu,p}[V] - \epsilon_{\nu,p'}[V]} \chi_{\nu,p'}[V](z).$$

## Iterations

After computing the Gâteaux-derivative of the density and developing calculations, we are led to a Poisson-like equation

$$-\operatorname{div}(\epsilon_R \nabla V^{\text{new}}) + \int_0^{l_z} \mathcal{A}[V^{\text{old}}](z, \zeta) V^{\text{new}}(\zeta) d\zeta$$

$$= -\frac{q}{\epsilon_0} (N[V^{\text{old}}] - N_D) + \int_0^{l_z} \mathcal{A}[V^{\text{old}}](z, \zeta) V^{\text{old}}(\zeta) d\zeta,$$

where  $\mathcal{A}[V]$  is essentially the Gâteaux-derivative of the functional  $P[V]$ .

# The iterations

## Derivatives

The Gâteaux-derivatives of the eigenproperties are needed:

$$d\epsilon_{\nu,p}(V, U) = -q \int U(\zeta) |\chi_{\nu,p}[V](\zeta)|^2 d\zeta$$

$$d\chi_{\nu,p}(V, U) = -q \sum_{p' \neq p} \frac{\int U(\zeta) \chi_{\nu,p}[V](\zeta) \chi_{\nu,p'}[V](\zeta) d\zeta}{\epsilon_{\nu,p}[V] - \epsilon_{\nu,p'}[V]} \chi_{\nu,p'}[V](z).$$

## Iterations

After computing the Gâteaux-derivative of the density and developping calculations, we are led to a Poisson-like equation

$$-\operatorname{div}(\epsilon_R \nabla V^{\text{new}}) + \int_0^{l_z} \mathcal{A}[V^{\text{old}}](z, \zeta) V^{\text{new}}(\zeta) d\zeta$$

$$= -\frac{q}{\epsilon_0} (N[V^{\text{old}}] - N_D) + \int_0^{l_z} \mathcal{A}[V^{\text{old}}](z, \zeta) V^{\text{old}}(\zeta) d\zeta,$$

where  $\mathcal{A}[V]$  is essentially the Gâteaux-derivative of the functional  $P[V]$ .

# Comparison Newton-Raphson vs. Gummel

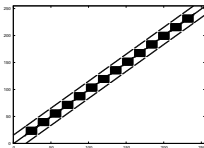
## Gummel

$$-\operatorname{div}(\varepsilon_R \nabla V^{new}) + \frac{q}{\varepsilon_0} N \frac{q}{k_B T_L} V^{new} = -\frac{q}{\varepsilon_0} (N - N_D) + \frac{q}{\varepsilon_0} N \frac{q}{k_B T_L} V^{old}$$

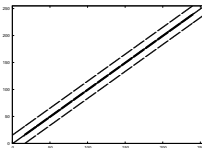
## Newton-Raphson

$$-\operatorname{div}(\varepsilon_R \nabla V^{new}) + \int_0^{l_z} \mathcal{A}(z, \zeta) V^{new}(\zeta) d\zeta = -\frac{q}{\varepsilon_0} (N - N_D) + \int_0^{l_z} \mathcal{A}(z, \zeta) V^{old}(\zeta) d\zeta$$

## Comparison

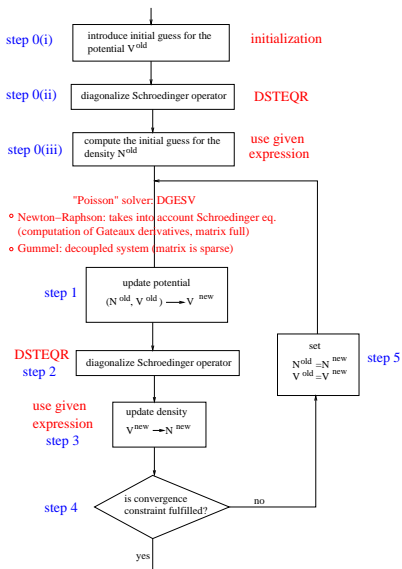


(g) Newton-Raphson



(h) Gummel

# Framework



# Outline

- 1 The model
  - Introduction
  - Modelling
- 2 Numerical schemes
  - Iterative schemes for the Schrödinger-Poisson block
  - **Solvers for Schrödinger and Poisson**
  - Numerical methods for the BTE
  - Parallelization
- 3 Experiments
  - Newton vs. Gummel
  - Equilibria
  - Time-dependent simulations
  - Plasma oscillations (from the one-valley solver)

# Numerical methods

We need to solve the Schrödinger eigenvalue problem and Poisson equations.

## The Schrödinger equation

Equation

$$-\frac{\hbar^2}{2} \frac{d}{dz} \left[ \frac{1}{m_{z,\nu}} \frac{d\chi_{\nu,p}}{dz} \right] - q(V + V_c) \chi_{\nu,p} = \epsilon_{\nu,p} \chi_{\nu,p}$$

is discretized by alternate finite differences for the derivatives then the symmetric matrix is diagonalized by a LAPACK routine called DSTEQR.

## The Poisson equation

We need to solve equations like

$$-\operatorname{div} [\epsilon_R \nabla V] + \int_0^{t_z} \mathcal{A}(z, \zeta) V(\zeta) d\zeta = \mathcal{B}(z).$$

The derivatives are discretized by finite differences in alternate directions, the integral is computed via trapezoid rule and the linear system (banded) is solved by means of a LAPACK routine called ?GBSV.

# Numerical methods

We need to solve the Schrödinger eigenvalue problem and Poisson equations.

## The Schrödinger equation

Equation

$$-\frac{\hbar^2}{2} \frac{d}{dz} \left[ \frac{1}{m_{z,\nu}} \frac{d\chi_{\nu,p}}{dz} \right] - q(V + V_c) \chi_{\nu,p} = \epsilon_{\nu,p} \chi_{\nu,p}$$

is discretized by alternate finite differences for the derivatives then the symmetric matrix is diagonalized by a LAPACK routine called DSTEQR.

## The Poisson equation

We need to solve equations like

$$-\text{div} [\epsilon_R \nabla V] + \int_0^{t_z} \mathcal{A}(z, \zeta) V(\zeta) d\zeta = \mathcal{B}(z).$$

The derivatives are discretized by finite differences in alternate directions, the integral is computed via trapezoid rule and the linear system (banded) is solved by means of a LAPACK routine called ?GBSV.



# Numerical methods

We need to solve the Schrödinger eigenvalue problem and Poisson equations.

## The Schrödinger equation

Equation

$$-\frac{\hbar^2}{2} \frac{d}{dz} \left[ \frac{1}{m_{z,\nu}} \frac{d\chi_{\nu,p}}{dz} \right] - q(V + V_c) \chi_{\nu,p} = \epsilon_{\nu,p} \chi_{\nu,p}$$

is discretized by alternate finite differences for the derivatives then the symmetric matrix is diagonalized by a LAPACK routine called DSTEQR.

## The Poisson equation

We need to solve equations like

$$-\text{div} [\epsilon_R \nabla V] + \int_0^{l_z} \mathcal{A}(z, \zeta) V(\zeta) d\zeta = \mathcal{B}(z).$$

The derivatives are discretized by finite differences in alternate directions, the integral is computed via trapezoid rule and the linear system (banded) is solved by means of a LAPACK routine called ?GBSV.

# Outline

- 1 The model
  - Introduction
  - Modelling
- 2 Numerical schemes
  - Iterative schemes for the Schrödinger-Poisson block
  - Solvers for Schrödinger and Poisson
  - **Numerical methods for the BTE**
  - Parallelization
- 3 Experiments
  - Newton vs. Gummel
  - Equilibria
  - Time-dependent simulations
  - Plasma oscillations (from the one-valley solver)

# Adimensionalization of the wave-vector space

The wave-vector space is adimensionalized by a change of variables into ellipsoidal variables, in order to better integrate the scattering operator and to have a simple expression for the kinetic energy and related magnitudes.

## Ellipsoidal coordinated

The wave-vector for the  $\nu^{\text{th}}$  valley reads:

$$(\tilde{k}_x, \tilde{k}_y) = \frac{\sqrt{m_e \kappa_B T_L}}{\hbar} \sqrt{2w(1 + \alpha_\nu w)} (\sqrt{m_{x,\nu}} \cos(\phi), \sqrt{m_{y,\nu}} \sin(\phi)).$$

## The Jacobian

The magnitude  $s_\nu(w)$  represents the dimensionless Jacobian of the change of variables in the wave-vector space:

$$s_\nu(w) = \left| \det \frac{\partial (k_x, k_y)}{\partial (w, \phi)} \right| = \sqrt{m_{x,\nu} m_{y,\nu}} (1 + 2\alpha_\nu w).$$

# Adimensionalization of the wave-vector space

The wave-vector space is adimensionalized by a change of variables into ellipsoidal variables, in order to better integrate the scattering operator and to have a simple expression for the kinetic energy and related magnitudes.

## Ellipsoidal coordinated

The wave-vector for the  $\nu^{\text{th}}$  valley reads:

$$(\tilde{k}_x, \tilde{k}_y) = \frac{\sqrt{m_e \kappa_B T_L}}{\hbar} \sqrt{2w(1 + \alpha_\nu w)} (\sqrt{m_{x,\nu}} \cos(\phi), \sqrt{m_{y,\nu}} \sin(\phi)).$$

## The Jacobian

The magnitude  $s_\nu(w)$  represents the dimensionless Jacobian of the change of variables in the wave-vector space:

$$s_\nu(w) = \left| \det \frac{\partial (k_x, k_y)}{\partial (w, \phi)} \right| = \sqrt{m_{x,\nu} m_{y,\nu}} (1 + 2\alpha_\nu w).$$

# BTE in ellipsoidal coordinates

Let the flux coefficients

$$a_{\nu}^1(w, \phi) = \frac{\sqrt{2w(1 + \alpha_{\nu}w)} \cos(\phi)}{\sqrt{m_{x,\nu}}} \frac{1}{1 + 2\alpha_{\nu}w}$$

$$a_{\nu,p}^2(x, w, \phi) = -\frac{\partial \epsilon_{\nu,p}}{\partial x}(x) \frac{1}{1 + 2\alpha_{\nu}w} \frac{\sqrt{2w(1 + \alpha_{\nu}w)} \cos(\phi)}{\sqrt{m_{x,\nu}}}$$

$$a_{\nu,p}^3(x, w, \phi) = \frac{\partial \epsilon_{\nu,p}}{\partial x}(x) \frac{\sin(\phi)}{\sqrt{m_{x,\nu}} \sqrt{2w(1 + \alpha_{\nu}w)}}.$$

Conservation-law form

$$\frac{\partial \Phi_{\nu,p}}{\partial t} + \frac{\partial}{\partial x} [a_{\nu}^1 \Phi_{\nu,p}] + \frac{\partial}{\partial w} [a_{\nu,p}^2 \Phi_{\nu,p}] + \frac{\partial}{\partial \phi} [a_{\nu,p}^3 \Phi_{\nu,p}] = \mathcal{Q}_{\nu,p}[\Phi]s(w)$$

# BTE in ellipsoidal coordinates

Let the flux coefficients

$$a_{\nu}^1(w, \phi) = \frac{\sqrt{2w(1 + \alpha_{\nu}w)} \cos(\phi)}{\sqrt{m_{x,\nu}}} \frac{1}{1 + 2\alpha_{\nu}w}$$

$$a_{\nu,p}^2(x, w, \phi) = -\frac{\partial \epsilon_{\nu,p}}{\partial x}(x) \frac{1}{1 + 2\alpha_{\nu}w} \frac{\sqrt{2w(1 + \alpha_{\nu}w)} \cos(\phi)}{\sqrt{m_{x,\nu}}}$$

$$a_{\nu,p}^3(x, w, \phi) = \frac{\partial \epsilon_{\nu,p}}{\partial x}(x) \frac{\sin(\phi)}{\sqrt{m_{x,\nu}} \sqrt{2w(1 + \alpha_{\nu}w)}}.$$

Conservation-law form

$$\frac{\partial \Phi_{\nu,p}}{\partial t} + \frac{\partial}{\partial x} [a_{\nu}^1 \Phi_{\nu,p}] + \frac{\partial}{\partial w} [a_{\nu,p}^2 \Phi_{\nu,p}] + \frac{\partial}{\partial \phi} [a_{\nu,p}^3 \Phi_{\nu,p}] = \mathcal{Q}_{\nu,p}[\Phi]s(w)$$

# Runge-Kutta time integration

We use a Runge-Kutta time discretization.

## Runge-Kutta

We advance in time by the third order Total Variation Diminishing Runge-Kutta scheme: if the evolution equation reads

$$H_{\nu,p}(\Phi) := -\frac{\partial}{\partial x} [a_{\nu,p}^1 \Phi_{\nu,p}] - \frac{\partial}{\partial w} [a_{\nu,p}^2 \Phi_{\nu,p}] - \frac{\partial}{\partial \phi} [a_{\nu,p}^3 \Phi_{\nu,p}] + \mathcal{Q}_{\nu,p}[\Phi]s(w)$$

(no explicit time-dependency), then

- 1  $\Phi_{\nu,p}^{(1)} = \Delta t H_{\nu,p}(\Phi^n)$
- 2  $\Phi_{\nu,p}^{(2)} = \frac{3}{4} \Phi_{\nu,p}^n + \frac{1}{4} \Phi_{\nu,p}^{(1)} + \frac{1}{4} \Delta t H_{\nu,p}(\Phi^{(1)})$
- 3  $\Phi^{n+1} = \frac{1}{3} \Phi_{\nu,p}^n + \frac{2}{3} \Phi_{\nu,p}^{(2)} + \frac{2}{3} H_{\nu,p}(\Phi^{(2)})$

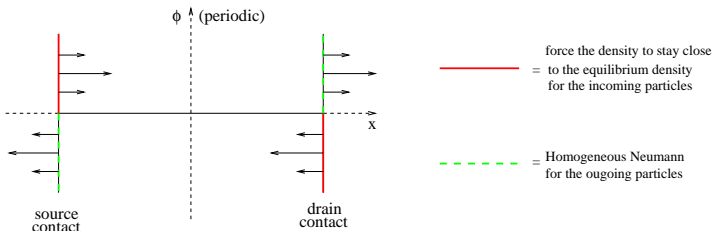
# Boundary conditions for the BTE

## $x$ -derivative

We use inflow/outflow b.c.: for the incoming particles

$$f_{\nu,p}(t, -x, w, \phi) = \frac{\rho_{\nu,p}^{eq}(0)}{\rho_{\nu,p}(0)} f_{\nu,p}(t, 0, w, \phi),$$

so as to have  $\int_{\mathbb{R}^2} f_{\nu,p}(t, 0, k) dk = \rho_{\nu,p}^{eq}$ , thus fulfilling the electrical neutrality constraint. For the outgoing particles, just use homogeneous Neumann b.c.

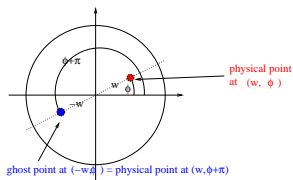




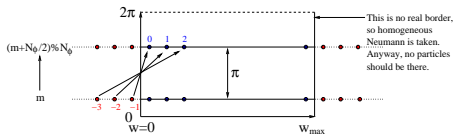
# Boundary conditions for the BTE

## w-derivative

$w = 0$  is no real boundary; ghost points at  $(-w, \phi)$  are physical points at  $(w, \phi + \pi)$ .  
At  $w = w_{max}$  there should be no particles, for properly chosen meshes: just use homogeneous Neumann b.c.



WAVE VECTOR VIEW



Ghost points for negative energy are physical points for a  $\pi$ -shifted angle.

(ENERGY, ANGLE)-VIEW



# Integrating the scattering operator

## Elastic phenomena

$$\begin{aligned} Q_{\nu,p}[\Phi]s_{\nu}(w) &= C_1^Q \sum_{p'} \frac{1}{W_{(\nu,p'),(\nu,p)}} \mathbb{I}_{\{\Gamma_0 \geq 0\}} \\ &\times \left[ s_{\nu}(w) \int_{\phi'=0}^{2\pi} \Phi_{\nu,p'}(\Gamma_0, \phi') d\phi' - 2\pi \Phi_{\nu,p} s_{\nu}(\Gamma_0) \right] \end{aligned}$$

## Energy gap

When electrons change their state from  $(\nu, p)$  to  $(\nu', p')$ , energy jumps appear:

$$\Gamma_0(x, w) = \epsilon_{\nu,p}^{tot}(x, w) - \epsilon_{\nu',p'}(x).$$

Remark, nevertheless, that they do not exchange energies with the phonons (elastic interaction).

# Integrating the scattering operator

Here go the formulae for the integration of the collisional operator in the ellipsoidal dimensionless variables.

## Inelastic phenomena

$$\begin{aligned}
 & Q_{\nu,p}[\Phi]s_{\nu}(w) \\
 = & C^{\mathcal{Q}}s_{\nu}(w) \sum_{\nu',p'} \frac{\gamma_{\nu' \rightarrow \nu} N_{\nu' \rightarrow \nu}}{W_{(\nu',p'),(\nu,p)}} \mathbb{I}_{\{\Gamma_- \geq 0\}} \int_{\phi'=0}^{2\pi} \Phi_{\nu',p'}(\Gamma_-, \phi') d\phi' \\
 + & C^{\mathcal{Q}}s_{\nu}(w) \sum_{\nu',p'} \frac{\gamma_{\nu' \rightarrow \nu} (N_{\nu' \rightarrow \nu} + 1)}{W_{(\nu',p'),(\nu,p)}} \mathbb{I}_{\{\Gamma_+ \geq 0\}} \int_{\phi'=0}^{2\pi} \Phi_{\nu',p'}(\Gamma_+, \phi') d\phi' \\
 - & C^{\mathcal{Q}}2\pi \Phi_{\nu,p}(w, \phi) \sum_{\nu',p'} \frac{\gamma_{\nu \rightarrow \nu'} N_{\nu \rightarrow \nu'}}{W_{(\nu,p),(\nu',p')}} \mathbb{I}_{\{\Gamma_+ \geq 0\}} s_{\nu'}(\Gamma_+) \\
 - & C^{\mathcal{Q}}2\pi \Phi_{\nu,p}(w, \phi) \sum_{\nu',p'} \frac{\gamma_{\nu \rightarrow \nu'} (N_{\nu \rightarrow \nu'} + 1)}{W_{(\nu,p),(\nu',p')}} \mathbb{I}_{\{\Gamma_- \geq 0\}} s_{\nu'}(\Gamma_-)
 \end{aligned}$$

# Integrating the scattering operator

## Energy gaps

When electrons change their state from  $(\nu, p)$  to  $(\nu', p')$ , energy jumps appear:

$$\Gamma_{\pm}(x, w) = \epsilon_{\nu, p}^{\text{tot}}(x, w) - \epsilon_{\nu', p'}(x) \pm \frac{\hbar\omega}{\kappa_B T_L}$$

Remark that, for inelastic interactions, they exchange energies  $\hbar\omega$  with the phonons.

## Occupation numbers

The occupation numbers read

$$N_{\nu \rightarrow \nu'} = \frac{\sqrt{\frac{m_{x, \nu} m_{y, \nu}}{m_{x, \nu'} m_{y, \nu'}}} \frac{1+2\alpha_{\nu}}{1+2\alpha_{\nu'}} e^{\frac{\hbar\omega}{\kappa_B T_L}} + 1}{\left( e^{\frac{\hbar\omega}{\kappa_B T_L}} + 1 \right) \left( e^{\frac{\hbar\omega}{\kappa_B T_L}} - 1 \right)},$$

for intra-valley phenomena ( $\gamma_{\nu \rightarrow \nu'} = 0$  for  $\nu' \neq \nu$ ), reduce to the well-known

$$N = \frac{1}{e^{\frac{\hbar\omega}{\kappa_B T_L}} - 1}.$$

# Outline

- 1 The model
  - Introduction
  - Modelling
- 2 Numerical schemes
  - Iterative schemes for the Schrödinger-Poisson block
  - Solvers for Schrödinger and Poisson
  - Numerical methods for the BTE
  - **Parallelization**
- 3 Experiments
  - Newton vs. Gummel
  - Equilibria
  - Time-dependent simulations
  - Plasma oscillations (from the one-valley solver)

# Parallelization of the transport/collision integration

## The Runge-Kutta scheme

The scheme to advance in time

$$H_{\nu,p}(\Phi) = -\frac{\partial}{\partial x} [a_{\nu}^1 \Phi_{\nu,p}] - \frac{\partial}{\partial w} [a_{\nu,p}^2 \Phi_{\nu,p}] - \frac{\partial}{\partial \phi} [a_{\nu,p}^3 \Phi_{\nu,p}] + Q_{\nu,p}[\Phi]s(w)$$

$$\Phi_{\nu,p}^{(1)} = \Delta t H_{\nu,p}(\Phi^n)$$

$$\Phi_{\nu,p}^{(2)} = \frac{3}{4} \Phi_{\nu,p}^n + \frac{1}{4} \Phi_{\nu,p}^{(1)} + \frac{1}{4} \Delta t H_{\nu,p}(\Phi^{(1)})$$

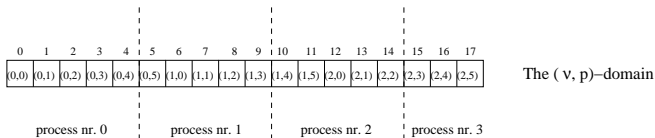
$$\Phi_{\nu,p}^{n+1} = \frac{1}{3} \Phi_{\nu,p}^n + \frac{2}{3} \Phi_{\nu,p}^{(2)} + \frac{2}{3} H_{\nu,p}(\Phi^{(2)})$$

is very local in the  $(\nu, p)$ -space: only the integration of the scattering operator  $Q_{\nu,p}[\Phi]s(w)$  requires information from other valleys and subbands.

# Parallelization of the transport/collision integration

## 1D block decomposition in the $(\nu, p)$ -space

We consider  $(\nu, p)$  as just one dimension and use MPI to exchange data following a 1D block distribution:



The information is gathered after each Runge-Kutta stage.



# Parallelization of the Schrödinger diagonalization

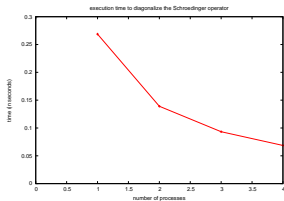
## The Schrödinger equation

In the eigenvalue problem,  $x$  only acts as a parameter:

$$-\frac{\hbar^2}{2} \frac{d}{dz} \left[ \frac{1}{m_{z,\nu}} \frac{d\chi_{\nu,p}[V]}{dz} \right] - q(V + V_c) \chi_{\nu,p}[V] = \epsilon_{\nu,p}[V] \chi_{\nu,p}[V].$$

## 1D block decomposition in the $x$ -space

We perform a simple 1D block decomposition in the  $x$ -domain: each process diagonalizes its set of equations, then the information is gathered (we use MPI). This way, we observe a  $\frac{1}{N_p}$ -decrease in the computational times:



# Parallelization of ?GBSV

## The goal

The goal is not the reduction of the computational times in the solution of the linear system, rather in assembling the matrix, which is the bottleneck of this block.

## ScaLAPACK's P?GBSV

The banded matrix for ?DGBSV has dimension  $(2 \cdot KL + 2 \cdot KU + 1) \times (N_x \cdot N_z)$ . The parallel version, requires cutting in the  $(N_x \cdot N_z)$ -dimension, i.e. a decomposition by column blocks.

## 1D block decomposition in the $(x, z)$ -space

We consider the  $(x, z)$ -space as a 1D space and perform a block decomposition (same strategy as for the  $(\nu, p)$ -decomposition):

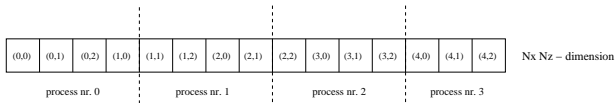


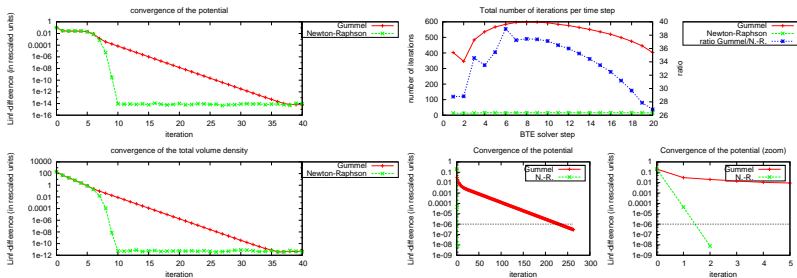
Figure: In this example  $(N_x, N_z) = (5, 3)$  and  $N_p = 4$ .

# Outline

- 1 The model
  - Introduction
  - Modelling
- 2 Numerical schemes
  - Iterative schemes for the Schrödinger-Poisson block
  - Solvers for Schrödinger and Poisson
  - Numerical methods for the BTE
  - Parallelization
- 3 Experiments
  - **Newton vs. Gummel**
  - Equilibria
  - Time-dependent simulations
  - Plasma oscillations (from the one-valley solver)

# Number of iterations

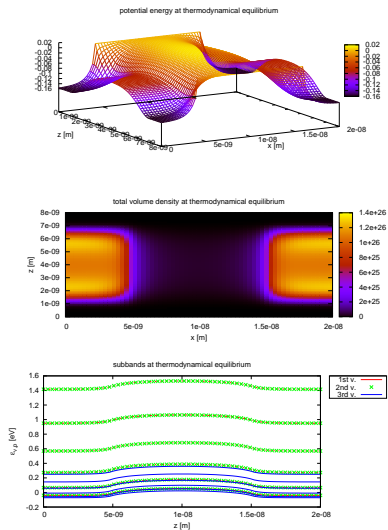
Newton schemes require much less iterations than Gummel in order to compute the thermodynamical equilibrium and any update of the potential; the results are the same up to machine error.



# Outline

- 1 The model
  - Introduction
  - Modelling
- 2 Numerical schemes
  - Iterative schemes for the Schrödinger-Poisson block
  - Solvers for Schrödinger and Poisson
  - Numerical methods for the BTE
  - Parallelization
- 3 Experiments
  - Newton vs. Gummel
  - **Equilibria**
  - Time-dependent simulations
  - Plasma oscillations (from the one-valley solver)

# Thermodynamical equilibrium: three-valley case



# Outline

- 1 The model
  - Introduction
  - Modelling
- 2 Numerical schemes
  - Iterative schemes for the Schrödinger-Poisson block
  - Solvers for Schrödinger and Poisson
  - Numerical methods for the BTE
  - Parallelization
- 3 Experiments
  - Newton vs. Gummel
  - Equilibria
  - **Time-dependent simulations**
  - Plasma oscillations (from the one-valley solver)

# Long-time behavior

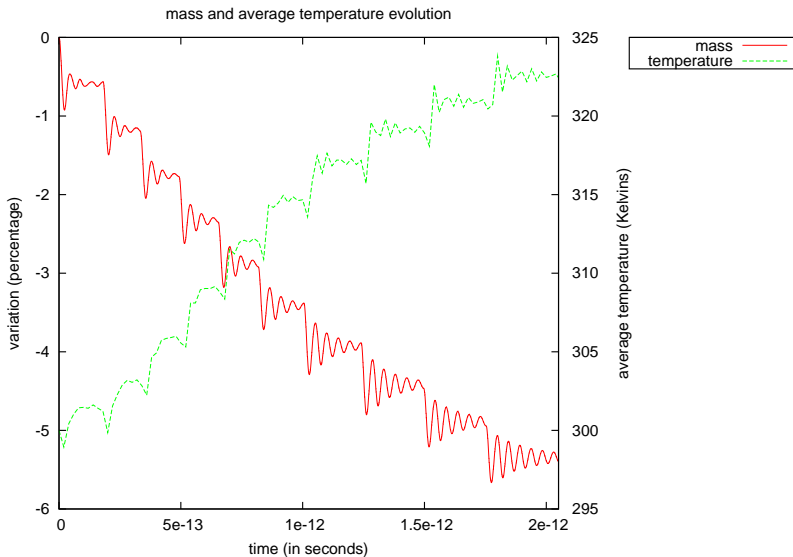
We propose now some results relative to the long-time behavior of the system.



# Outline

- 1 The model
  - Introduction
  - Modelling
- 2 Numerical schemes
  - Iterative schemes for the Schrödinger-Poisson block
  - Solvers for Schrödinger and Poisson
  - Numerical methods for the BTE
  - Parallelization
- 3 Experiments
  - Newton vs. Gummel
  - Equilibria
  - Time-dependent simulations
  - Plasma oscillations (from the one-valley solver)

# Mass and temperature oscillations



# Numerically-computed oscillations

The plasma frequency is given by

$$\omega_p = \sqrt{\frac{q^2 N_e}{\epsilon_R \epsilon_0 m_*}}$$

$N_D^{high}$ ( $\times 10^{26} m^{-3}$ )	$\epsilon_R$	$m_*$	$N_e$ ( $\times 10^{26} m^{-3}$ )	$\omega_{num}$ ( $\times 10^{14} s^{-1}$ )	$\omega_p$ ( $\times 10^{14} s^{-1}$ )	Ratio $\frac{\omega_{num}}{\omega_{ref}}$	Expected Ratio
1	11.7	0.5	.400	$\omega_{ref} = 1.344$	1.475	1	/
2	11.7	0.5	.783	2.051	2.064	1.52	$\sqrt{2}$
4	11.7	0.5	1.544	2.813	2.899	2.09	2
1	5.85	0.5	.400	1.848	2.086	1.37	$\sqrt{2}$